Journal of Non-Crystalline Solids 501 (2018) 85–92

Contents lists available at ScienceDirect

Journal of Non-Crystalline Solids

journal homepage: www.elsevier.com/locate/jnoncrysol

Control of self-powdering phenomenon in ferroelastic β′-$Gd_2(MoO_4)_3$ crystallization in boro-tellurite glasses

Mikiya Kotaka[a], Tsuyoshi Honma[a], Takayuki Komatsu[a,*], Kenji Shinozaki[b], Mario Affatigato[c], Ralf Müller[d]

[a] Department of Materials Science and Technology, Nagaoka University of Technology, 1603-1 Kamitomioka-cho, Nagaoka 940-2188, Japan
[b] National Institute of Advanced Industrial Science and Technology (AIST), 1-8-31 Midorigaoka, Ikeda, Osaka 563-8577, Japan
[c] Physics Department, Coe College, 1220 1st Ave NE, Cedar Rapids, IA 52402, USA
[d] BAM Federal Institute for Materials Research and Testing, 12489 Berlin, Germany

ARTICLE INFO

Keywords:
Crystallization
Self-powdering phenomenon
Periodic refractive index change
Stress
Ferroelastic β′-$Gd_2(MoO_4)_3$

ABSTRACT

Glasses with compositions of $21Gd_2O_3$-$63MoO_3$-(16-x)B_2O_3-xTeO_2 (mol%) (x = 0, 2, 4, 8) were prepared using a conventional melt quenching technique, and the crystallization behavior of ferroelastic β′-$Gd_2(MoO_4)_3$ crystals was examined to clarify the mechanism of self-powdering phenomenon and to design bulk crystallized glasses. It was found that the self-powdering phenomenon appeared significantly during the crystallization at temperatures near the crystallization peak temperature, but the phenomenon is suppressed in the crystallization at temperatures much higher than the glass transition temperature. It was also found that the substitution of TeO_2 for B_2O_3 in the base glasses suppresses the self-powdering phenomenon and consequently bulk crystallized glasses were obtained in the glass with x = 8 mol%. The densities at room temperature of the base glasses are d = 4.755–4.906 g/cm^3, being much higher than the value of d = 4.555 g/cm^3 for β′-$Gd_2(MoO_4)_3$ crystal. It is proposed that the stresses in the inside of crystals induced by large density differences (i.e., large molar volume differences) between the glassy phase and crystals might be relaxed effectively in the glasses containing TeO_2 with weak Te—O bonds and fragile character.

1. Introduction

The controlled crystallization of glasses is a method for the fabrication of transparent and dense condensed materials with desired shapes and functions, and so far, various functional glass-ceramics have been proposed through the design and control of glass composition, nucleation and crystal growth [1–4]. One of the strong motivations for the development of glass-ceramics is to improve mechanical properties of glasses, e.g., improvements of hardness and fracture toughness due to the design of the microstructure of crystal/glass composites. A good example is the glass-ceramics based on the Li_2O-Al_2O_3-SiO_2 system, which have excellent optical and mechanical functions with the achievements of nano-crystallization and nearly zero thermal expansion coefficients [1,2]. Another attractive motivation is to develop optical, electrical, and magnetic active glass-ceramics in which active crystals such as ferroelectric $LiNbO_3$ and $Sr_xBa_{1-x}Nb_2O_6$ are included [3–7]. It should be also emphasized that the crystallization processing of glasses is becoming more and more important as an approach for a deep understanding of the nano-scale heterogeneous structure in glasses [4,8].

The present authors' group has been trying to develop glass-ceramics consisting of β′-$Gd_2(MoO_4)_3$ crystals (designated here as β′-GMO crystals) [9–17], because β′-GMO crystal exhibits ferroelastic and ferroelectric properties, i.e., the so-called multiferroic crystal [18–23] and multiferroic β′-GMO has potential applications in piezoelectric, electro-optic, electro-acoustic, frequency converting, and other fields [22,24]. Tsukada et al. [10] found an extremely unique and curious phenomenon in the formation of β′-GMO crystals in $21.25Gd_2O_3$-$63.75MoO_3$-$15B_2O_3$ glass (designated here as GM15B glass). That is, crystals formed in the crystallization break into small pieces with triangular prism or pyramidal shapes having a length of 50–150 μm spontaneously during the crystallization upon heating an electric furnace, not during the cooling in air. They called this phenomenon “self-powdering phenomenon” [10]. To the best of our knowledge, such a self-powdering phenomenon has not been observed in the crystallization of any other glasses. Wang et al. [17] noticed the fact that the glasses based on the system of Gd_2O_3-MoO_3-B_2O_3 have larger densities at room temperature compared with β′-GMO crystals and proposed that such differences in the density might induce the accumulation of extremely large stresses

* Corresponding author.
E-mail address: komatsu@mst.nagaokaut.ac.jp (T. Komatsu).

https://doi.org/10.1016/j.jnoncrysol.2017.12.006
Received 19 September 2017; Received in revised form 14 November 2017; Accepted 2 December 2017
Available online 07 December 2017

in the inside of GMO crystals, eventually causing the breaking of crystals. At this moment, however, the origin or mechanism of self-powdering phenomenon observed experimentally has not been clarified in detail. If we can inhibit the self-powdering phenomenon through the design of glass composition and heat treatment conditions, it might be possible to develop bulk glass-ceramics (not powders), and such bulk glass-ceramics might be expected as new materials having extremely large stresses in the inside without breaking.

The purpose of this study is to develop bulk glass-ceramics consisting of ferroelastic β′-GMO crystals without inducing the self-powdering phenomenon in Gd_2O_3-MoO_3-B_2O_3-TeO_2 glasses. We focused on the host glass formers of the so-called strong glass-forming oxide of B_2O_3 and fragile glass-forming oxide of TeO_2. It is known that the binary system of (1-x)TeO_2-xB_2O_3 shows the glass-formation in the range of x = 0.05–0.30 and also there is no chemical interaction between TeO_2 and B_2O_3, providing the crystallization of only α-TeO_2 phase [25,26]. Even in Na_2O-TeO_2-B_2O_3 glasses, there is no experimental evidence for the possible formation of B-O-Te linkages [27]. Generally, B_2O_3-based glasses consist of tetrahedral BO_4 and trigonal BO_3 units, and TeO_2-based glasses include trigonal bi-pyramidal TeO_4 and trigonal pyramidal TeO_3 units. Although the structure of Gd_2O_3-MoO_3-B_2O_3-TeO_2 glasses has not been clarified as of this moment, the presence of both B_2O_3 and TeO_2 might lead to complex speciation in the glass structure, i.e., the formation of BO_3, BO_4, TeO_4, and TeO_3 structural units, and consequently to the change in connectivity and rigidity of the network. Furthermore, it is known that the binary MoO_3-B_2O_3 system does not have any wide glass-forming region [28], but, the binary MoO_3-TeO_2 system shows a wide glass-forming region [29]. It is, therefore, expected that boro-tellurite glasses containing both B_2O_3 and TeO_2 would have unique and complicated glass structures leading to the different stress relaxation behaviors between the glassy phase and β′-GMO crystals in the crystallization of β′-GMO in Gd_2O_3-MoO_3-B_2O_3-TeO_2 glasses. In this study, we found that the self-powdering phenomenon is largely suppressed by the substitution of TeO_2 for B_2O_3, leading to the synthesis of bulk glass-ceramics with β′-GMO.

2. Experimental

Glasses with the compositions of $21Gd_2O_3$-$63MoO_3$-(16-x)B_2O_3-xTeO_2 (mol%) (x = 0, 2, 4 and 8) were prepared using a conventional melt quenching technique. Commercial powders of reagent grade Gd_2O_3, MoO_3, B_2O_3, and TeO_2 were used as starting materials, and their mixtures were melted in an alumina crucible at 1100 °C for 30 min in an electric furnace. The melts were poured onto an iron plate and pressed to a thickness of ~1.5 mm by another iron plate. The glass transition (T_g) and crystallization peak (T_p) temperatures were determined using differential thermal analysis (DTA) at heating rate of 10 K/min. The as-quenched glasses were annealed at ~T_g for 30 min to release internal stresses and then polished mechanically to a mirror finish with CeO_2 powders. Powdered glasses with the size of about 20 μm were prepared by using an agate motor in hand. Densities of the glasses at room temperature (d) were determined with the Archimedes method using distilled water as an immersion liquid. We cannot find any problems with water resistance of the glasses.

The glasses were heat-treated at different temperatures in an electric furnace, and the crystalline phases present in the crystallized samples were identified by X-ray diffraction (XRD) analysis (CuKα radiation) and Raman scattering spectra (Tokyo Instruments Co., Nanofinder; Ar^+ laser with a wavelength of λ = 488 nm). Some glasses with a plate shape were heated on the heat stage, and the change in the morphology of crystals was observed with a polarized optical microscope (POM).

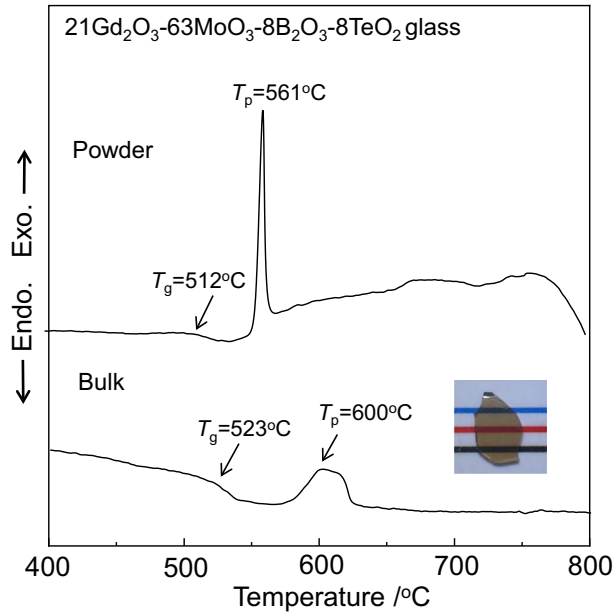

Fig. 1. DTA curves for the bulk and powdered samples of $21Gd_2O_3$-$63MoO_3$-$8B_2O_3$-$8TeO_2$ glass. Heating rate was 10 K/min. T_g and T_p are the glass transition and crystallization peak temperatures, respectively. The optical photograph for the bulk glass is also shown. (For interpretation of the references to color in this figure, the reader is referred to the web version of this article.)

3. Results and discussion

3.1. Self-powdering phenomenon in Gd_2O_3-MoO_3-B_2O_3-TeO_2 glasses

The glasses of $21Gd_2O_3$-$63MoO_3$-(16-x)B_2O_3-xTeO_2 (mol%) (x = 0, 2, 4 and 8) prepared in this study are designated here as GdMo16B glass for x = 0, GdMo14B2Te for x = 2, GdMo12B4Te for x = 4, and GdMo8B8Te for x = 8. The DTA curves for the bulk and powder samples of GdMo8B8Te are shown in Fig. 1 as an example. This glass has a brown color, and its optical photograph is shown in Fig. 1. The glass shows endothermic dips due to the glass transition and exothermic peaks due to the crystallization, providing the values of T_g = 523 °C and T_p = 600 °C for the bulk sample and T_g = 512 °C and T_p = 561 °C for the powder sample. It is noted that the difference in crystallization peak temperature is large, being typical for surface induced crystallization. Similar DTA profiles are observed for other samples, and the values of T_g and T_p for the bulk samples are summarized in Table 1. It is seen that the value of T_g tends to decrease with the substitution of TeO_2 for B_2O_3. Furthermore, it should be pointed that the value of T_g = 523 °C for the bulk sample in the glass with x = 8 ($8TeO_2$) is different from the value of T_g = 512 °C for the powder sample (see in Fig. 1). A similar trend was observed in other $21Gd_2O_3$-$63MoO_3$-(16-x)B_2O_3-xTeO_2 (mol%) glasses with 2 and 4, i.e., T_g = 533 °C (bulk) and

Table 1
Chemical compositions, values of the glass transition T_g (bulk sample), crystallization peak T_p (bulk sample) temperatures, density d, and molar volume V_m for $21Gd_2O_3$-$63MoO_3$-(16-x)B_2O_3-xTeO_2 (mol%) (x = 0, 2, 4 and 8) glasses prepared in the study. The glasses are designated here as GaMo16B glass for x = 0, GaMo14B2Te for x = 2, GaMo12B4Te for x = 4, and GaMo8B8Te for x = 8. The values of d and V_m for β′-$Gd_2(MoO_4)_3$ crystal are also included.

Sample #	T_g (°C) (± 2 °C)	T_p (°C) (± 2 °C)	d (g/cm^3) (± 0.004)	V_m (cm^3/mol)
GdMo16B	537	584	4.755	37.42
GdMo14B2Te	533	605	4.742	37.90
GdMo12B4Te	530	608	4.806	37.77
GdMo8B8Te	523	600	4.906	37.74
β′-$Gd_2(MoO_4)_3$	–	–	4.555	43.60

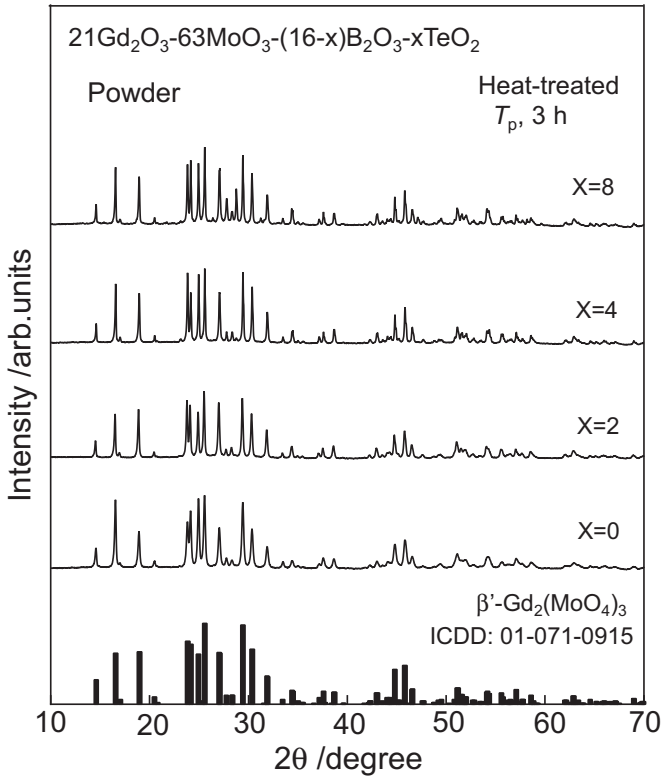

Fig. 2. XRD patterns at room temperature for the powdered samples crystallized at peak temperature T_p for 3 h in $21Gd_2O_3$-$63MoO_3$-(16-x)B_2O_3-xTeO_2 glasses with x = 0, 2, 4, and 8. The peaks are assigned to the β′-$Gd_2(MoO_4)_3$ crystalline phase.

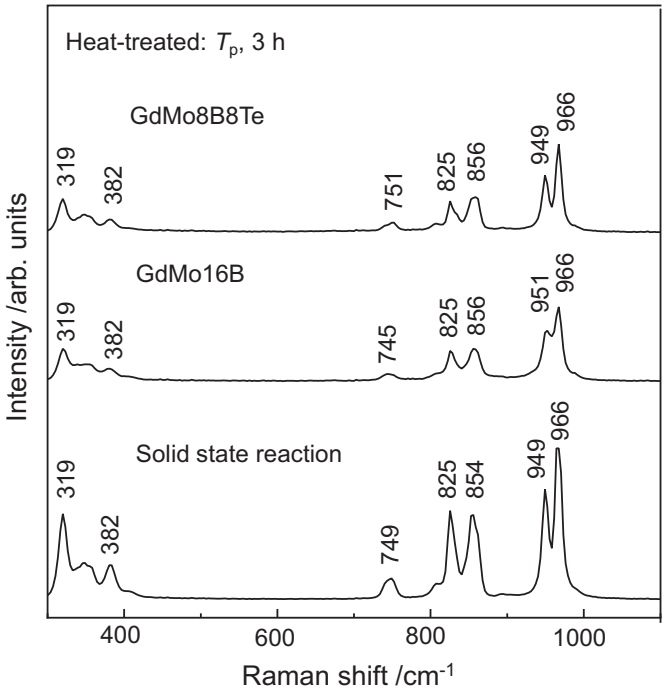

Fig. 3. Raman scattering spectra at room temperature for the crystallized (at T_p for 3 h) samples of GdMo16B and GdMo8B8Te. The spectrum for the sample obtained by a solid state reaction (sintered at 1000 °C for 24 h in air) is also shown.

T_g = 541 °C (powder) for the glass with x = 2 and T_g = 530 °C (bulk) and T_g = 524 °C (powder) for the glass with x = 4. The glass of $21Gd_2O_3$-$63MoO_3$-$16B_2O_3$ (mol%) with no TeO_2, however, showed the same value of T_g = 537 °C for the bulk and powder samples. At this moment, the origin of the difference in the glass transition temperature for the bulk and powder samples in the glasses with both B_2O_3 and TeO_2 is unclear. The values of density d measured are also shown in Table 1, indicating an increase in d with increasing TeO_2 content.

The glasses of GdMo16B, GdMo14B2Te, GdMo12B4Te, and GdMo8B8Te were heat-treated at T_p for 3 h in air, and the XRD patterns for the crystallized samples (the samples were pulverized after heat treatments) at room temperature are shown in Fig. 2. In these experiments, the samples were cooled in an electric furnace after the heat treatments. It is seen that all crystallized samples show the formation of β′-$Gd_2(MoO_4)_3$ crystals (ICDD: 01-071-0915), irrespective of the content ratio of TeO_2/B_2O_3. The Raman scattering spectra at room temperature for the crystallized (at T_p for 3 h) samples of GdMo16B and GdMo8B8Te are shown in Fig. 3 together with the spectrum for the sample obtained by a solid state reaction (sintered at 1000 °C for 24 h in air). These Raman scattering spectra also demonstrate the formation of β′-$Gd_2(MoO_4)_3$ crystals for the crystallized samples in $21Gd_2O_3$-$63MoO_3$-(16-x)B_2O_3-xTeO_2 glasses [10,12]. In the ferroelastic state of β′-$Gd_2(MoO_4)_3$ crystal [18–22], spontaneous strains are present within crystals. The Curie temperature of $Gd_2(MoO_4)_3$ crystals in the phase transition from the ferroelastic state (β′-$Gd_2(MoO_4)_3$) with an optically birefringence property ($n_a = n_b$ = 1.85 and n_c = 1.90) [19,23] to the paraelastic state (β-$Gd_2(MoO_4)_3$) with an optically uniaxial property is T_c = 163 °C [20]. β-$Gd_2(MoO_4)_3$ has a tetragonal structure with $a = b$ = 1.0419 nm and c = 1.0636 nm at 200 °C, and β′-$Gd_2(MoO_4)_3$ has an orthorhombic structure with a = 1.0388 nm, b = 1.0426 nm, and c = 1.0709 nm at room temperature. Thus, the difference in their crystal structure parameters is small. It is, therefore, considered that crystals formed in the crystallization (heat-treatment temperature: ~600 °C) of Gd_2O_3-$MoO_3B_2O_3$-TeO_2 glasses would be paraelastic β-$Gd_2(MoO_4)_3$ crystals with no spontaneous strains and during the cooling in an electric furnace after heat treatments, paraelastic β-$Gd_2(MoO_4)_3$ crystals transform into ferroelastic β′-$Gd_2(MoO_4)_3$ crystals. Abe et al. [30] also proposed that the initial crystalline phase formed in the crystallization of $21.15Sm_2O_3$-$63.75MoO_3$-$15B_2O_3$ is paraelectric β-$Sm_2(MoO_4)_3$.

The optical photographs at room temperature for the samples obtained by heat treatments of the glasses at T_p for 3 h in an electric furnace in air are shown in Fig. 4. As seen in Fig. 4, the original bulk glasses with a plate shape of GdMo16B, GdMo14B2Te break into small pieces. That is, the self-powdering phenomenon is observed in the crystallization of β′-$Gd_2(MoO_4)_3$ crystals not only in GdMo16B but also in GdMo14B2Te glasses. It should be again emphasized that the breaking into small pieces is taking place spontaneously during the heating stage of an electric furnace, not during the cooling after the crystallization. On the other hand, the breaking into small pieces during the crystallization was not observed in GdMo12B4Te and GdMo8B8Te glasses, although the former glass plate has been deformed during crystallization. However, observing more in detail, it was found that the heat-treated sample for GdMo12B4Te glass breaks into some pieces easily after touching. In GdMo8B8Te glass, a rigid bulk glass-ceramics was obtained. It should be pointed out that a plate-shape glass breaks into two plate-shape glass-ceramics after heat treatments and the breaking is taking place almost at the center plane. These results indicate that the self-powdering phenomenon observed in Gd_2O_3-MoO_3-B_2O_3 glasses is suppressed due to the substitution of TeO_2 for B_2O_3.

The polarization optical microscope (POM) photographs for crystal grains (piece) obtained by heat treatment at T_p for 3 h in an electric furnace are shown in Fig. 5. It is found the grains have triangular prism or pyramidal shapes. In GdMo16B glass, their color is not uniform over the whole region of the grain, but the bright and dark regions indicate periodic refractive index changes. The widths of the bright region (high refractive index) and the dark region (low refractive index) are about 5.5 μm and about 3.5 μm, respectively [10]. It has been proposed that the orientation of $(MoO_4)^{2-}$ tetrahedra in β′-$Gd_2(MoO_4)_3$ crystals

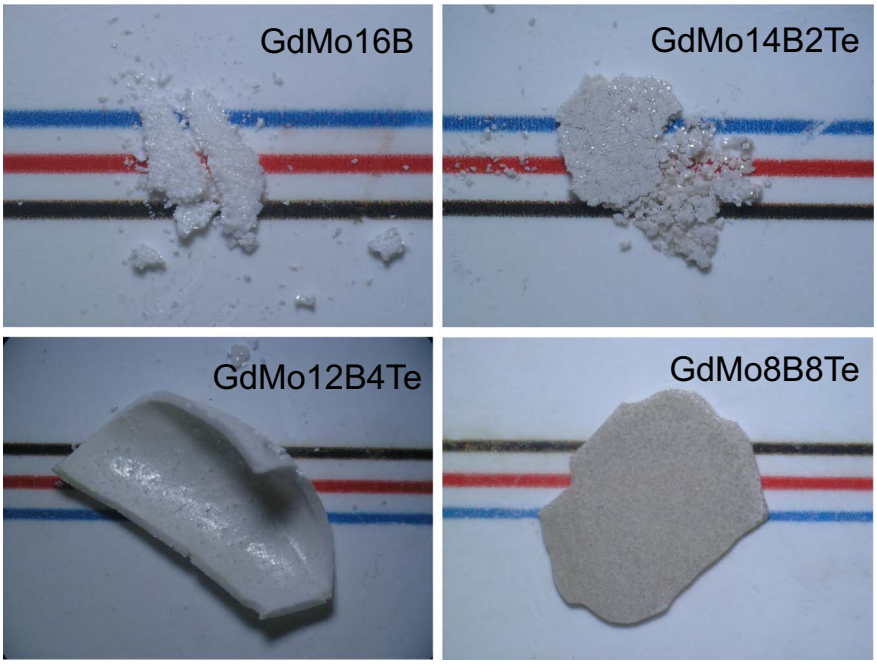

Fig. 4. Optical photographs at room temperature for the samples obtained by heat treatments at peak temperature T_p for 3 h in $21Gd_2O_3$-$63MoO_3$-(16-x)B_2O_3-xTeO_2 glasses with x = 0, 2, 4, and 8.

changes gradually and periodically along the crystal growth direction due to spontaneous strains in β′-$Gd_2(MoO_4)_3$ crystals [10,16]. As seen in Fig. 5, however, such a periodic refractive index change was not observed in the crystal grains formed in the crystallization of GdMo12B4Te and GdMo8B8Te glasses. The results shown in Figs. 4 and 5 suggest strongly that the self-powdering phenomenon and the appearance of periodic refractive index change are closely related each other.

As reported in the previous papers [10,17] and as confirmed in the present study, the self-powdering phenomenon in GdMo16B is observed in the glasses heat-treated at around the crystallization peak temperatures T_p of ~600 °C. We examined the effect of heat treatment temperatures on the self-powdering phenomenon, in particular about heat treatments at high temperatures, using the following experiment; the GdMo16B glass was put in directly into an electric furnace heated to 800 °C, i.e., not a gradual heating. The optical photograph for the sample heated at 800 °C for 15 min is shown in Fig. 6. It was confirmed from XRD analysis at room temperature that β′-$Gd_2(MoO_4)_3$ crystals are formed in this heat treatment. It is seen that the crystallized sample is deformed, but does break into small pieces. However, this crystallized sample also breaks into some pieces easily after touching. Furthermore, it was found that any periodic refractive index change similar to the pattern shown in Fig. 5 (a) was not induced in the grains as shown in Fig. 6. It is, therefore, concluded that the self-powdering phenomenon in GdMo16B glass is suppressed through crystallization at high temperatures. We also examined whether the periodic refractive index change appears or not in β′-$Gd_2(MoO_4)_3$ crystal grains synthesized by a conventional solid state reaction for the mixture of Gd_2O_3 and MoO_3. As

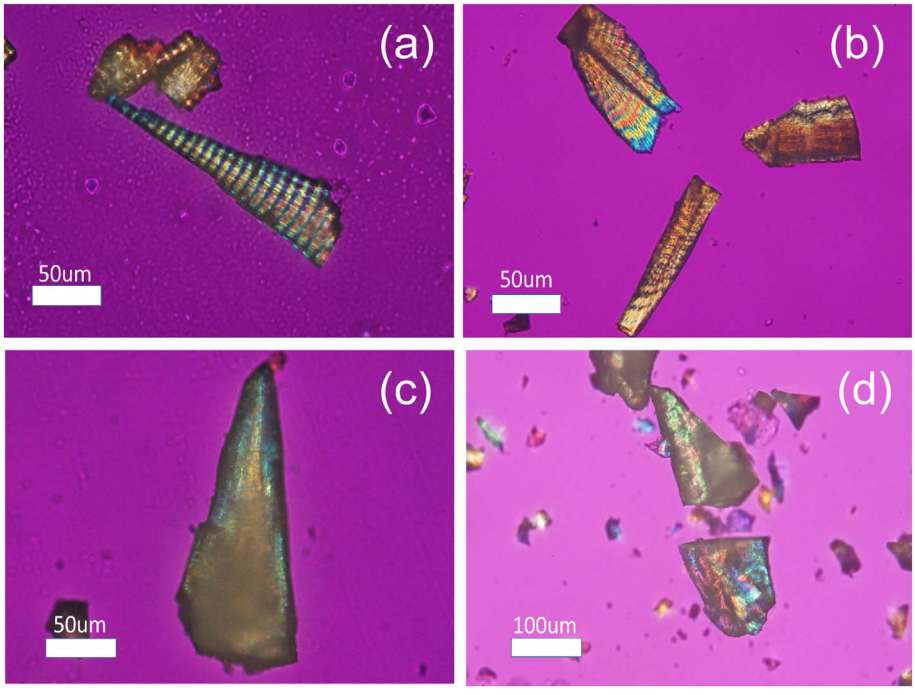

Fig. 5. Polarized optical photographs at room temperature for the samples obtained by heat treatments at peak temperature T_p for 3 h in $21Gd_2O_3$-$63MoO_3$-(16-x)B_2O_3-xTeO_2 glasses. (a) for x = 0, (b) for x = 2, (c) for x = 4, and (d) for x = 8.

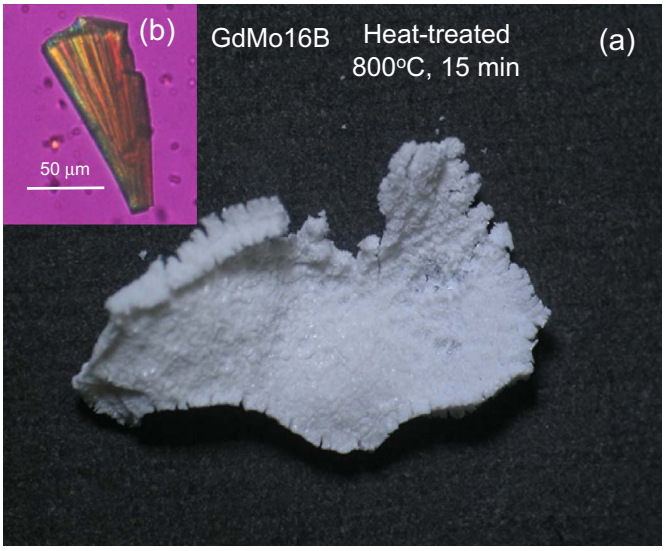

Fig. 6. Optical photograph (a) and polarized optical photograph (b) at room temperature for the sample obtained by a heat treatment at 800 °C for 15 min in $21Gd_2O_3$-$63MoO_3$-$16B_2O_3$ glass.

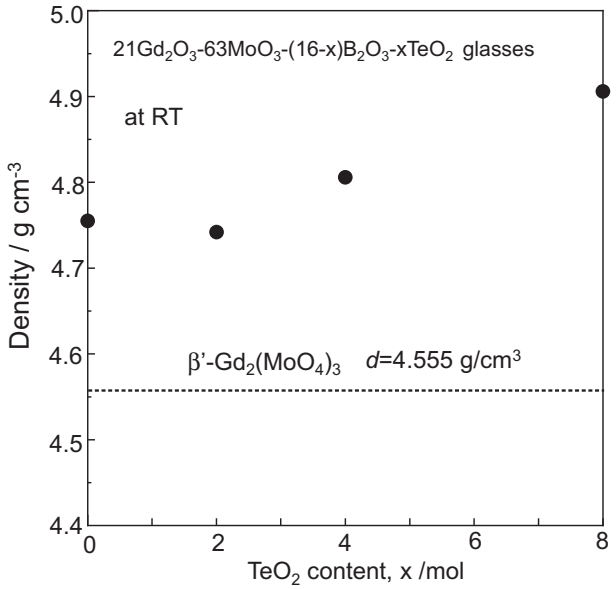

Fig. 7. Densities at room temperature for $21Gd_2O_3$-$63MoO_3$-(16-x)B_2O_3-xTeO_2 glasses obtained in the present study and β′-$Gd_2(MoO_4)_3$ crystal [31].

a result, it was confirmed that the periodic refractive index change did not appear. These results including the results shown in Figs. 4 to 6 propose strongly that the self-powdering phenomenon and also the appearance of periodic refractive index change in β′-$Gd_2(MoO_4)_3$ crystals are unique features in the crystals formed through the processing of the crystallization of glasses.

3.2. Mechanism of self-powdering phenomenon

The results clarified in the present study (Figs. 1 to 6) provide us the following four important points on the crystallization of ferroelastic β′-$Gd_2(MoO_4)_3$ crystals in $21Gd_2O_3$-$63MoO_3$-(16-x)B_2O_3-xTeO_2 (mol%) (x = 0, 2, 4 and 8) glasses: 1) the initial crystalline phase formed in the crystallization of the glasses is β-$Gd_2(MoO_4)_3$ crystals, and this crystalline phase transforms into ferroelastic β′-$Gd_2(MoO_4)_3$ crystalline phase during the cooling to room temperature, 2) the self-powdering phenomenon appeared significantly during the crystallization at temperatures near the crystallization peak temperature, but this phenomenon is suppressed in the crystallization at temperatures much higher than the glass transition temperature, 3) the self-powdering phenomenon during crystallization is suppressed by the substitution of TeO_2 for B_2O_3 in the base glasses, 4) the appearance of periodic refractive index changes in the grains of β′-$Gd_2(MoO_4)_3$ crystals is closely related to the self-powdering phenomenon.

It should be emphasized that the nucleation and crystal growth of β-$Gd_2(MoO_4)_3$ is taking place in Gd_2O_3-MoO_3-B_2O_3-TeO_2 glasses containing two different glass-forming oxides of B_2O_3 and TeO_2. The self-powdering phenomenon indicates clearly that extremely large stresses causing the breaking of crystals are accumulated in the inside of β-$Gd_2(MoO_4)_3$ crystals. In this point of view, Wang et al. [17] focused on the difference in the density (d) between β′-$RE_2(MoO_4)_3$ crystals (RE: Sm. GD, Dy) and the base glasses of RE_2O_3-MoO_3-B_2O_3 and found that the base glasses have larger densities at room temperature compared with β′-$RE_2(MoO_4)_3$ crystals, which is a unique feature in the RE_2O_3-MoO_3-B_2O_3 system compared with the crystallization of other glass systems. They proposed that such differences in the density might induce the accumulation of extremely large stresses in the inside of $RE_2(MoO_4)_3$ crystals, eventually causing the breaking of crystals into small pieces [17].

The values of densities at room temperature for $21Gd_2O_3$-$63MoO_3$-(16-x)B_2O_3-xTeO_2 (mol%) (x = 0, 2, 4 and 8) glasses are shown in Fig. 7. It is seen that the density increases with increasing the substation of TeO_2 for B_2O_3, e.g., d = 4.755 g/cm^3 for $21Gd_2O_3$-$63MoO_3$-$16B_2O_3$ glass (x = 0) and d = 4.906 g/cm^3 for $21Gd_2O_3$-$63MoO_3$-$8B_2O_3$-$8TeO_2$ glass with x = 8. The value of d = 4.555 g/cm^3 for β′-$Gd_2(MoO_4)_3$ crystal [31] is also indicated in Fig. 7. Here, we used the densities of the base glasses and β′-$Gd_2(MoO_4)_3$ crystal at room temperature, because their densities at high temperatures such as 600 and 800 °C have not been measured. It is found from Fig. 7 that all base glasses have large density values compared with β′-$Gd_2(MoO_4)_3$ crystal. Even in $21Gd_2O_3$-$63MoO_3$-(16-x)B_2O_3-xTeO_2 glasses and even at high temperatures, it is, therefore, expected that large stresses would be accumulated in the inside of $Gd_2(MoO_4)_3$ crystals formed in the glasses, as proposed by Wang et al. [17]. As can be seen in Fig. 7, the difference in the densities of the glass with x = 8 (d = 4.906 g/cm^3) and β′-$Gd_2(MoO_4)_3$ crystal is large compared with the case of the glass with x = 0 (d = 4.755 g/cm^3) and β′-$Gd_2(MoO_4)_3$ crystal. The values of molar volume V_m ($= M_w/d$: M_w is the molecular weight) for the glasses are summarized in Table 1, together with the value for β′-$Gd_2(MoO_4)_3$ crystal. It is seen that the glasses have considerably small V_m values compared with β′-$Gd_2(MoO_4)_3$ crystal, e.g. V_m = 37.74 cm^3/mol for GdMo8B8Te glass and V_m = 43.60 cm^3/mol for β′-$Gd_2(MoO_4)_3$ crystal. These large differences in the molar volume also suggest that large stresses would be induced at the interface between β′-$Gd_2(MoO_4)_3$ crystals and the surrounding glassy phase, as discussed from the viewpoint of density. As found in this study (Fig. 4), however, the self-powdering phenomenon is observed more clearly in the glass with x = 0, but not in the glass with x = 8. It should be pointed out that the difference in the molar volume between GdMo16B glass (x = 0) with V_m = 37.42 cm^3/mol and GdMo8B8Te (x = 8) with V_m = 37.74 cm^3/mol is not large. In other words, in order to clarify the mechanism of the self-powdering phenomenon, other factors must be considered besides the density (or molar volume) difference in the based glasses and $Gd_2(MoO_4)_3$ crystal.

The fact obtained in the present study, i.e., the self-powdering phenomenon during crystallization is suppressed by the substitution of TeO_2 for B_2O_3 in $21Gd_2O_3$-$63MoO_3$-(16-x)B_2O_3-xTeO_2 glasses, suggests that the degree (value) of accumulated stresses in the inside of $Gd_2(MoO_4)_3$ crystals, which is created from the density (or molar volume) difference in the glassy phase and the formed β-$Gd_2(MoO_4)_3$ crystals, changes depending on the glassy phase. That is, the so-called stress relaxation might be considered for the stresses created from the density difference. It is well known that TeO_2-based glasses are

classified into the so-called fragile glasses, because their viscosities and also Vickers hardness decrease sharply around the glass transition temperature [32–34]. On the other hand, B_2O_3-based glasses have been considered to be strong glasses [35], and it is well known that the single bond strength of B—O bonds in B_2O_3 is extremely large compared with that of Te—O bonds in TeO_2 [36,37]. Indeed, as seen in Table 1, the glass transition temperature in $21Gd_2O_3$-$63MoO_3$-(16-x)B_2O_3-xTeO_2 glasses decreases with the substitution of TeO_2 for B_2O_3. Considering these structural and bonding features in B_2O_3-based and TeO_2-based glasses, the relaxation of stresses created from the density differences in the glassy phase and β-$Gd_2(MoO_4)_3$ crystals would be more significant in the glasses with high TeO_2 contents, decreasing the accumulation of stresses in the inside of β-$Gd_2(MoO_4)_3$ crystals and consequently suppressing the self-powdering phenomenon. The stress relaxation at the interface between the glassy phase and β-$Gd_2(MoO_4)_3$ crystals would be also large at high temperatures, because the viscosity of the glassy phase decreases with increasing temperature and the stress at the interface would dissipate effectively to the surrounding low viscous glassy phase. Indeed, as shown in Fig. 6, the self-powdering phenomenon is suppressed in the crystallization at a high temperature of 800 °C. It is known that the $Ba_2TiGe_2O_8$ crystalline phase (designated as BTG) with the so-called fresnoite ($Ba_2TiSi_2O_8$)-type structure (non-centrosymmetric tetragonal structure) exhibits ferroelastic behavior [38,39]. The density of BTG crystal is 4.84 g/cm^3 and that of BTG glass is 4.74 g/cm^3, indicating that the BTG crystalline phase has a larger density compared with the corresponding BTG glass [38,39]. Indeed, in the crystallization of BaO-TiO_2-GeO_2 glasses, any self-powdering phenomenon has not been observed [40,41], being a complete contrast to the case of the crystallization of ferroelastic β′-$Gd_2(MoO_4)_3$ in Gd_2O_3-MoO_3-B_2O_3 glasses.

In order to understand more deeply the suppression of self-powdering phenomenon in $21Gd_2O_3$-$63MoO_3$-(16-x)B_2O_3-xTeO_2 glasses, we also need to light the structure of these glasses. Altering the proportions of TeO_2/B_2O_3 in the glasses could change the ratio of BO_3 and BO_4, and thus, it is expected the change in connectivity and rigidity of the network in the glasses containing both TeO_2 and B_2O_3, and consequently, the change in stress relaxation behaviors. Halimah et al. [42] proposed that the increasing of TeO_2 content in the binary TeO_2-B_2O_3 glasses results in an increase in the cross-link density due to the transformation of BO_3 into BO_4 units and the transformation of TeO_4 to TeO_3 units. It should be pointed out that $21Gd_2O_3$-$63MoO_3$-(16-x)B_2O_3-xTeO_2 glasses contain only the total amount of 16 mol% in the glass-forming oxides of B_2O_3 and TeO_2. These glasses are, therefore, regarded as really unique glasses from the viewpoint of chemical composition. It is desired to study the structure of $21Gd_2O_3$-$63MoO_3$-(16-x)B_2O_3-xTeO_2 glasses by using techniques such as ^{11}B MAS-NMR.

It is known that in the as-grown state, ferroelastic β′-$Gd_2(MoO_4)_3$ single crystal always contains twins with the *a*- and *b*-axes interchanged. Furthermore, there are also multiple domains of nearly parallel orientation with a small (~1°) rotation around the *c*-axis [20]. The axis of domains in β′-$Gd_2(MoO_4)_3$ is directed along [110] crystallographic direction, and it is known that β′-$Gd_2(MoO_4)_3$ crystals cleave in [110] direction on (100) plane [43]. If a large mechanical stress is applied to a paraelastic β-$Gd_2(MoO_4)_3$ crystal with a tetragonal structure ($a = b \neq c$), some distortion in the crystal structure would be expected and consequently, the β-$Gd_2(MoO_4)_3$ crystal structure might be close to the β′-$Gd_2(MoO_4)_3$ crystal structure. In other words, in β-$Gd_2(MoO_4)_3$ crystals formed in the crystallization of $21Gd_2O_3$-$63MoO_3$-(16-x)B_2O_3-xTeO_2 glasses and also surrounded by other glassy phases consisting of B_2O_3 and TeO_2, twins and domains with a *c*-axis rotation might be formed. However, in the case of a small mechanical strength (stress) against β-$Gd_2(MoO_4)_3$ crystals, such twins and domains would not be expected. This model might be applied to explain the fact that the self-powdering phenomenon during crystallization is suppressed by the substitution of TeO_2 for B_2O_3 in $21Gd_2O_3$-$63MoO_3$-(16-x)B_2O_3-xTeO_2 glasses.

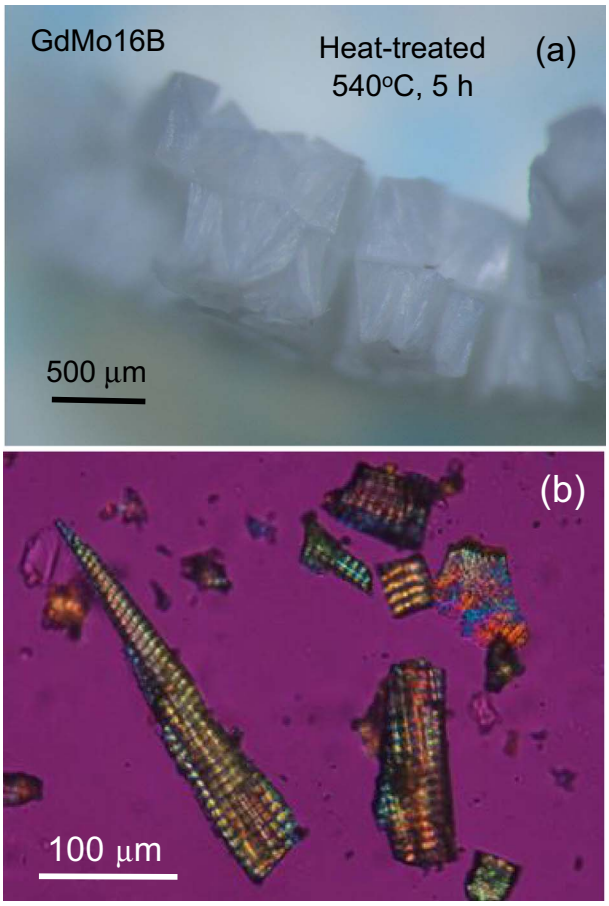

Fig. 8. Optical photograph (a) and polarized optical photograph (b) at room temperature for the sample obtained by a heat treatment at 540 °C for 5 h in $21Gd_2O_3$-$63MoO_3$-$16B_2O_3$ glass.

The optical photograph at room temperature for the cross-section of the sample heat-treated at 540 °C for 5 h in $21Gd_2O_3$-$63MoO_3$-$16B_2O_3$ glass and POM photograph for the grains obtained from the sample are shown in Fig. 8 (a) and (b), respectively. It should be pointed out that the crystalline phase at room temperature in this crystallized sample is β′-$Gd_2(MoO_4)_3$ and the grains show periodic refractive index changes as similar to Fig. 5 (a). The widths of the bright region and the dark region in Fig. 8 are about 5.3 μm and about 3 μm, respectively. Unique cleavage (cracks) and planes are observed, and these features might be similar to the fracture behavior of β′-$Gd_2(MoO_4)_3$ single crystal, although the crystallographic cleavage direction and plane miller indices in the crystallized sample have not been determined as of this moment. The XRD patterns at room temperature for the samples heat-treated at 599 °C for 3 h in $21Gd_2O_3$-$63MoO_3$-$8B_2O_3$-$8TeO_2$ glass are shown in Fig. 9. A rigid bulk glass-ceramics was obtained. However, it was found that the plate-shape crystallized sample breaks into two sheets and the separation is taking place almost at the center plane of the original glass sample. Their photographs are also included in Fig. 9. The XRD patterns indicate that the crystalline phase at room temperature in the crystallized sample is β′-$Gd_2(MoO_4)_3$. Furthermore, it is found that highly *c*-axis oriented β′-$Gd_2(MoO_4)_3$ crystals are present at the original surface (outside: before breaking into two sheets) of the crystallized sample, suggesting the surface crystallization mechanism. On the other hand, such a high orientation is not confirmed at the new surface created after breaking, i.e., in the center part of crystallized sample. It is obvious that the growth of highly oriented β-$Gd_2(MoO_4)_3$ crystals starting from the front surface stops at the center part of the base glass because of the collision with other β-$Gd_2(MoO_4)_3$ crystals growing from the back surface. Such a collision would not form a strong chemical bonding

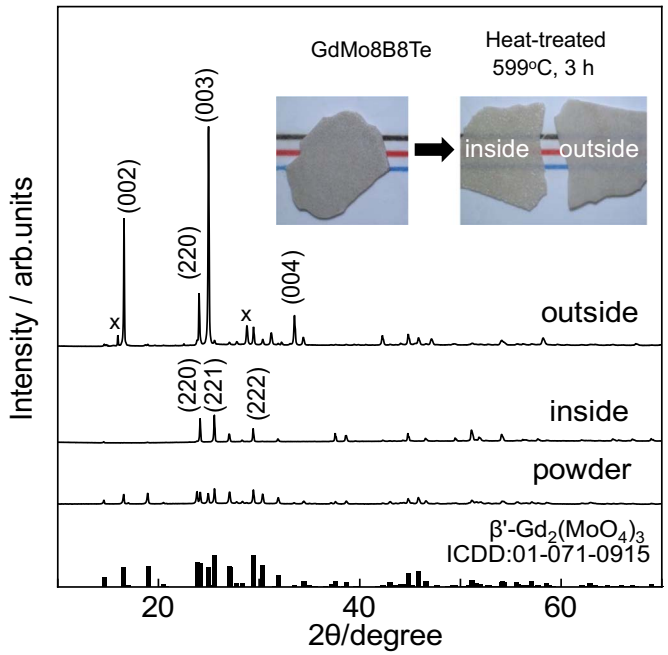

Fig. 9. XRD patterns at room temperature for the bulk sample crystallized at 599 °C for 3 h in $21Gd_2O_3$-$63MoO_3$-$8B_2O_3$-$8TeO_2$ glass. The bulk crystallized sample was separated into two plates, creating different two surfaces of the outside and the inside. The peaks are assigned to the β′-$Gd_2(MoO_4)_3$ crystalline phase. The peaks marked by "x" are not identified.

between β-$Gd_2(MoO_4)_3$ crystals growing from the different surfaces (the front and back surfaces). Recently, Takahashi et al. [44] reported the perfect surface crystallization of fresnoite $Ba_2TiSi_2O_8$ in 28BaO-$18TiO_2$-$54SiO_2$ glass, in which highly *c*-axis oriented $Ba_2TiSi_2O_8$ crystals grow from the front and back surfaces and stop at the center part of plate-shaped samples. It should be, however, pointed out that any breaking into two sheets has not been reported in their crystallized samples. In their study [44], the chemical composition of the base glass is 28BaO-$18TiO_2$-$54SiO_2$, indicating a large deviation from the chemical composition of $Ba_2TiSi_2O_8$. That is, it is expected that a large amount of the glassy phase with chemical compositions such as $4TiO_2$-$26SiO_2$ would be present even in the final stage (perfect surface crystallization) of crystallization in their glass and such a residual glassy phase would play the role of strong connections between $Ba_2TiSi_2O_8$ crystals growing from the different surfaces. On the other hand, in our present study, the chemical composition of $21Gd_2O_3$-$63MoO_3$-$8B_2O_3$-$8TeO_2$ glass is very close to that of $Gd_2(MoO_4)_3$, i.e., $21Gd_2O_3$-$63MoO_3$, and thus, the amount of the glassy phase is also small, i.e., $8B_2O_3$-$8TeO_2$. This would be one of the reasons for the appearance of the breaking into two sheets after the sufficient crystallization (Fig. 9) in our present study.

3.3. Origin of periodic refractive index changes

In the present study, it was clarified that the appearance of periodic refractive index changes in the grains of β′-$Gd_2(MoO_4)_3$ crystals is closely related to the self-powdering phenomenon. Ferroelastic β′-$Gd_2(MoO_4)_3$ crystal has an optical birefringence property, meaning that the periodic refractive index change shown in Figs. 5 (a) and 8 (b) is not induced by the mere formation of twins with the *a*- and *b*-axes interchanged, but the change in the *c*-axis direction is also required. In other words, the appearance of periodic refractive index changes indicates that the *c*-axis direction of β-$Gd_2(MoO_4)_3$ crystals formed in the crystallization of glasses changes periodically together with the crystal growth.

It would be worth summarizing the important points on the periodic refractive index change observed in the grains and also laser patterned lines of β′-$Gd_2(MoO_4)_3$ crystals, which were reported in the previous papers [10,14,16]. Tsukada et al. [10] found from the azimuthal dependence of second harmonic (SH) intensities and polarized micro-Raman scattering spectra that β′-$Gd_2(MoO_4)_3$ crystal in each grain is oriented and the orientation of $(MoO_4)^{2-}$ tetrahedral units changes periodically, providing periodic refractive index changes in grains. Suzuki et al. [16] demonstrated from transmission electron microscope observations that a gradual rotation of crystallographic axes takes place along the crystal growth direction (laser scanning direction) in β′-$(Sm,Gd)_2(MoO_4)_3$ crystal lines patterned by laser irradiations, providing the gradual rotation of $(MoO_4)^{2-}$ tetrahedral units. Wang et al. [14] found that the periodic degree of refractive index changes in the laser pattering of β′-$RE_2(MoO_4)_3$ crystal lines (RE: Sm, Gd, Tb, and Dy) depends on the kinds of RE^{3+} ions and the periodicity of refractive index changes, i.e., the distance between high and low refractive index changes, varies with the laser scanning speed and thus with the growth speed of β′-$RE_2(MoO_4)_3$ crystals. The most important key point for the appearance of periodic refractive index change in β′-$RE_2(MoO_4)_3$ crystals formed in the crystallization of RE_2O_3-MoO_3-B_2O_3 glasses is a rotation of the *c*-axis in β′-$RE_2(MoO_4)_3$ crystals.

As proposed in the Section 3.2, if a large mechanical stress is applied to a paraelastic β-$Gd_2(MoO_4)_3$ crystal with a tetragonal structure ($a = b \neq c$), some distortion in the crystal structure would be expected. Furthermore, if such a distortion results in the apparent rotation of the *c*-axis, a periodic refractive index change would be observed in a grain of β′-$Gd_2(MoO_4)_3$ crystal.

4. Conclusions

The glasses with the compositions of $21Gd_2O_3$-$63MoO_3$-(16-x)B_2O_3-xTeO_2 (mol%) (x = 0, 2, 4, 8) were prepared using a conventional melt quenching technique, and the crystallization behavior of ferroelastic β′-$Gd_2(MoO_4)_3$ crystals was examined to clarify the mechanism of self-powdering phenomenon and to design bulk crystallized glasses. It was found that the self-powdering phenomenon appeared significantly during the crystallization at temperatures near the crystallization peak temperature, but the phenomenon is suppressed in the crystallization at temperatures much higher than the glass transition temperature. It was also found that the substitution of TeO_2 for B_2O_3 in the base glasses suppresses the self-powdering phenomenon and consequently bulk crystallized glasses were obtained in the glass with x = 8 mol%. The periodic refractive index change observed in β′-$Gd_2(MoO_4)_3$ crystal particles also disappeared in the samples with TeO_2 contents of 4 and 8 mol%. The densities at room temperature of the base glasses are d = 4.755–4.906 g/cm^3, being much higher than the value of d = 4.555 g/cm^3 for β′-$Gd_2(MoO_4)_3$ crystal. It is proposed that the stresses in the inside of crystals induced by large density (or molar volume) differences between the glassy phase and crystals might be relaxed effectively in the glasses containing TeO_2 with weak Te—O bonds and fragile character.

Acknowledgment

This work was supported by JSPS KAKENHI Grant Numbers 15K13804 and 17H03387.

References

[1] W. Höland, G.H. Beall, Glass-Ceramic Technology, John Wiley & Sons, 2012.
[2] A. Sakamoto, S. Yamamoto, Int. J. Appl. Glas. Sci. (2010) 1237–1247.
[3] T. Komatsu, T. Honma, Int. J. Appl. Glas. Sci. 4 (2013) 125–135.
[4] T. Komatsu, J. Non-Cryst. Solids 428 (2015) 156–175.
[5] H. Jain, Ferroelectrics 306 (2004) 111–127.
[6] T. Yamazawa, T. Honma, H. Suematsu, T. Komatsu, J. Am. Ceram. Soc. 92 (2009) 2924–2930.
[7] T. Komatsu, K. Koshiba, T. Honma, J. Solid State Chem. 184 (2011) 411–418.

[8] Y. Takahashi, M. Osada, H. Masai, T. Fujiwara, Phys. Rev. B 79 (2009) 214204.
[9] R. Nakajima, M. Abe, Y. Benino, T. Fujiwara, H.G. Kim, T. Komatsu, J. Non-Cryst. Solids 353 (2007) 85–93.
[10] Y. Tsukada, T. Honma, T. Komatsu, J. Solid State Chem. 182 (2009) 2269–2273.
[11] Y. Tsukada, T. Honma, T. Komatsu, Appl. Phys. Lett. 94 (2009) 059901.
[12] F. Suzuki, T. Honma, T. Komatsu, J. Solid State Chem. 183 (2010) 909–914.
[13] F. Suzuki, T. Honma, T. Komatsu, Mater. Chem. Phys. 125 (2011) 377–381.
[14] Y. Wang, T. Honma, T. Komatsu, Mater. Chem. Phys. 133 (2012) 118–125.
[15] Y. Wang, T. Honma, Y. Doi, Y. Hinatsu, T. Komatsu, J. Ceram. Soc. Japan 121 (2013) 230–235.
[16] F. Suzuki, T. Honma, T. Komatsu, J. Phys. Chem. Solids 75 (2014) 954–958.
[17] Y. Wang, T. Honma, T. Komatsu, J. Ceram. Soc. Japan 122 (2014) 777–783.
[18] H.J. Borchardt, P.E. Bierstedt, Appl. Phys. Lett. 8 (1966) 50–52.
[19] K. Aizu, A. Kumada, H. Yumoto, S. Ashida, J. Phys. Soc. Japan 27 (1969) 511.
[20] E.T. Keve, S.C. Abrahams, J.L. Bernstein, J. Chem. Phys. 54 (1971) 3185–3194.
[21] K. Nassau, J.W. Shiever, E.T. Keve, J. Solid State Chem. 3 (1971) 411–419.
[22] H. Nishioka, W. Odajima, M. Tateno, K. Ueda, A.A. Kaminskii, A.V. Butashin, S.N. Bagayev, A.A. Pavlyuk, Appl. Phys. Lett. 70 (1997) 1366–1368.
[23] A. Kumada, Ferroelectrics 3 (1972) 115–123.
[24] L.A. Coldren, R.A. Lemons, Appl. Phys. Lett. 32 (1978) 129–131.
[25] E. Kashchieva, P. Hinkov, Y. Dimitriev, S. Miloshev, J. Mater. Sci. Lett. 13 (1994) 1760–1763.
[26] D. Yardimci, M. Celikbilek, A.E. Ersundu, S. Aydin, Mater. Chem. Phys. 137 (2013) 999–1006.
[27] D. Larink, H. Eckert, J. Non-Cryst. Solids 426 (2015) 150–158.
[28] M. Imaoka, J. Ceram. Soc. Japan 69 (1961) 282–306.
[29] T. Sekiya, N. Mochida, S. Ogawa, J. Non-Cryst. Solids 185 (1995) 135–144.
[30] M. Abe, Y. Benino, T. Fujiwara, T. Komatsu, R. Sato, J. Appl. Phys. 97 (2005) 123516.
[31] L.H. Brixner, P.E. Bierstedt, A.W. Sleight, M.S. Licis, Mater. Res. Bull. 6 (1971) 545–554.
[32] T. Watanabe, Y. Benino, K. Ishizaki, T. Komatsu, J. Ceram. Soc. Japan 107 (1999) 1140–1145.
[33] K. Aida, Y. Benino, V. Dimitrov, T. Komatsu, J. Am. Ceram. Soc. 83 (2000) 1192–1198.
[34] T. Watanabe, Y. Benino, T. Komatsu, J. Non-Cryst. Solids 286 (2001) 141–145.
[35] L. Cormier, G. Calas, B. Beuneu, Phys. Chem. Glasses: Eur. J. Sci. Technol. B 50 (2009) 195–200.
[36] V. Dimitrov, T. Komatsu, J. Chem. Tech. Metal. 50 (2015) 387–396.
[37] V. Dimitrov, T. Tasheva, T. Komatsu, Phys. Chem. Glasses: Eur. J. Sci. Technol. B 57 (2016) 285–290.
[38] M. Kimura, K. Doi, S. Nanamatsu, T. Kawamura, Appl. Phys. Lett. 23 (1973) 531–532.
[39] A. Halliyal, A. Safari, A.S. Bhalla, R.E. Newnham, L.E. Cross, J. Am. Ceram. Soc. 67 (1984) 331–335.
[40] Y. Takahashi, Y. Benino, T. Fujiwara, T. Komatsu, Appl. Phys. Lett. 81 (2002) 223–225.
[41] Y. Takahashi, Y. Benino, T. Fujiwara, T. Komatsu, J. Non-Cryst. Solids 316 (2003) 320–330.
[42] M.K. Halimah, H.A.A. Sidek, W.M. Daud, H. Zainul, Z.A. Talib, A.W. Zaidan, A.S. Zainal, H. Mansor, Am. J. Appl. Sci. 2 (2005) 1541–1546.
[43] P. Panfilov, Y.L. Gagarin, V.Ya. Shur, J. Mater. Sci. 34 (1999) 241–246.
[44] Y. Takahashi, Y. Yamazawa, R. Ihara, T. Fujiwara, Appl. Phys. Lett. 102 (2013) 191903.